

# Crack propagation in a glass particle-filled epoxy resin

## Part 2 *Effect of particle-matrix adhesion*

J. SPANOUDAKIS, R. J. YOUNG

*Department of Materials, Queen Mary College, Mile End Road, London E1 4NS, UK*

The investigation outlined in the preceding paper has been extended to cover the effect of particle/matrix adhesion upon crack propagation in an epoxy resin reinforced with spherical glass particles. The behaviour has again been interpreted in terms of crack pinning and blunting. It has again been shown that in the absence of blunting a critical crack opening displacement criterion can be applied. The strength of the particle/matrix interface is found to affect both the crack propagation behaviour and the appearance of the fracture surface. It is also found to have a profound effect upon the fracture strength of the composites. The best overall mechanical properties are obtained for composites containing particles treated with coupling agent.

### 1. Introduction

In the preceding paper [1] the effect of particle size and volume fraction upon crack propagation in an epoxy resin was investigated. It was shown that the behaviour could be explained principally in terms of crack pinning, with contributions from blunting and breakdown of the particle-matrix interface. In this second paper the analysis has been extended to cover the effect of changing the strength of the particle-matrix interface upon the fracture behaviour.

Over the years there have been several reports of the effect of particle/matrix adhesion upon fracture in brittle particle-filled polymers [2-10]. Although it is well established that improving adhesion at the interface increases the fracture strength of the composite [3-7] it is not entirely clear as to how this affects crack propagation. There have been reports of improving adhesion at the interface both increasing [8] and decreasing [9, 10] the fracture energy,  $G_{Ic}$ , for crack propagation in particle-reinforced composites.

With good adhesion it is found that the fracture strength of the composites is approximately the same as that of the unfilled matrices. On the other hand, with no surface pretreatments, or release agents, applied to the particles the strength

decreases with increasing volume fractions of filler particles [4]. This behaviour has been explained theoretically by Leidner and Woodhams [5] who were able to predict the dependence of the fracture strength of the composite upon the strength of the particle/matrix bond in particle-filled polyester resins. The theory has been also shown to work well for particle-filled epoxy resins and has enabled the strength of the bond to be determined [6].

In the case of crack propagation, Broutman and Sahu [9] suggested that the increase in  $G_{Ic}$  for weak adhesion may be due to interfacial debonding above and below the fracture plane whereas Brown [10] has argued that the toughness is due to debonded particles acting as voids and causing more local energy absorbing processes, such as plastic deformation, to take place. This present study is concerned with the effect of the strength of the interface upon both the mechanisms of crack propagation in particle-filled epoxy resins and the fracture strength of these materials.

### 2. Experimental details

#### 2.1. Materials and moulding

In order to compare this present study with the previous work [1] the same materials and moulding conditions were employed. The epoxy resin used

was Epikote 828 hardened with tetraethylene pentamine (TEPA) and reinforced with spherical glass particles (ballotini). However, in this case, only two particle sizes were used – ballotini with average diameters of 4.5 and 62  $\mu\text{m}$  – i.e. the smallest and largest diameters employed in the previous study [1]. The mixing and moulding were carried out as before except that before mixing the glass particles were given one of two surface treatments.

### 2.1.1. Improved adhesion

In order to increase the adhesion between the particles and matrix a silane adhesion promoter, A187, ( $\gamma$ -glycidoxypropyltrimethoxy-silane) supplied by Union Carbide was used. The glass particles were cleaned in isopropanol and dried at 100°C *in vacuo* for 1 h. They were then mixed with a 1% aqueous solution of A187 for 5 min. The excess solution was filtered off and the treated particles were heated for 1 h, *in vacuo*, at 110°C. To avoid agglomerations the treated particles were sieved before mixing with the resin.

### 2.1.2. Decreased adhesion

The adhesion between the epoxy resin and the particles was reduced by employing the release agent DC 1107 supplied by Dow Corning. After cleaning the glass particles they were mixed with a 1% solution of the release agent in methylene chloride. The solution was filtered and the particles heated at 250°C for about two hours. They were then sieved and mixed with the resin and hardener and moulded as before [1].

## 2.2. Mechanical testing and fractography

As in the previous investigation [1] crack propagation in the various composites was followed using the Double Torsion (DT) test-piece. This technique allows the critical stress intensity factor  $K_{Ic}$  to be determined from the critical load for crack propagation and the specimen dimensions [1]. The moulded sheets were cut into rectangular 3.9 mm thick plates, 60 mm long and 30 mm wide, placed in the DT rig and deformed in an Instron Universal testing machine at  $22 \pm 2^\circ\text{C}$  using crosshead speeds from 0.05 to 5 mm min<sup>-1</sup>. The critical stress intensity factor,  $K_{Ic}$  was determined from the maximum load and the specimen dimensions as described earlier [1].

The Young's modulus,  $E$ , for each type of composite was determined in flexure [1] and the

fracture energy,  $G_{Ic}$  calculated as before [1] using the relation

$$G_{Ic} \sim K_{Ic}^2/E. \quad (1)$$

The fracture strengths,  $\sigma_f$ , of each type of composite were also determined in flexure using unnotched specimens [6]. Six specimens were used for each composition and the strengths quoted are the average of these six values.

The fracture surfaces of all the specimens were examined in a scanning electron microscope (Jeol JXA-50A) operated at 15 kV, after they have been made conductive by sputter-coating with a thin layer of gold.

## 3. Results and discussion

### 3.1. Stability of crack propagation

It was found with both types of surface pretreatment, A187 and DC1107, that crack propagation was either continuous and stable or unstable and stick/slip, depending upon the composition and testing conditions. This behaviour is similar to that of the composites containing untreated particles but the detailed behaviour was found to depend upon the surface pretreatment as can be seen in Figs. 1 and 2. In these figures,  $K_{Ic}$  is plotted against crosshead speed for increasing volume fractions of 4.5  $\mu\text{m}$  diameter particles. The stability of crack propagation can be judged from the difference between the initiation and arrest values of  $K_{Ic}$ . Propagation is continuous for the pure resin and with high volume fractions of particles but it is unstable at intermediate volume fractions ( $V_p \sim 0.18$ ). Propagation is also more unstable at low crosshead speeds. It can be seen by comparing Figs. 1 and 2 that propagation is more unstable for the particles treated with release agent (DC1107) than for those treated with the coupling agent (A187). The difference between the initiation and arrest values of  $K_{Ic}$  are much larger for the composites containing DC1107 treated particles.

The stability of crack propagation in the composites containing treated particles is similar to that of unfilled epoxy resins [11] and composites containing untreated particles [1]. The transition to stable behaviour on increasing the crosshead speed suggests strongly that the instability is caused by blunting [12, 13]. The higher instability for the composite with release agent treated particles implies that debonding at the particle/matrix interface may lead to more blunting. This is discussed in more detail in Section 4.1.

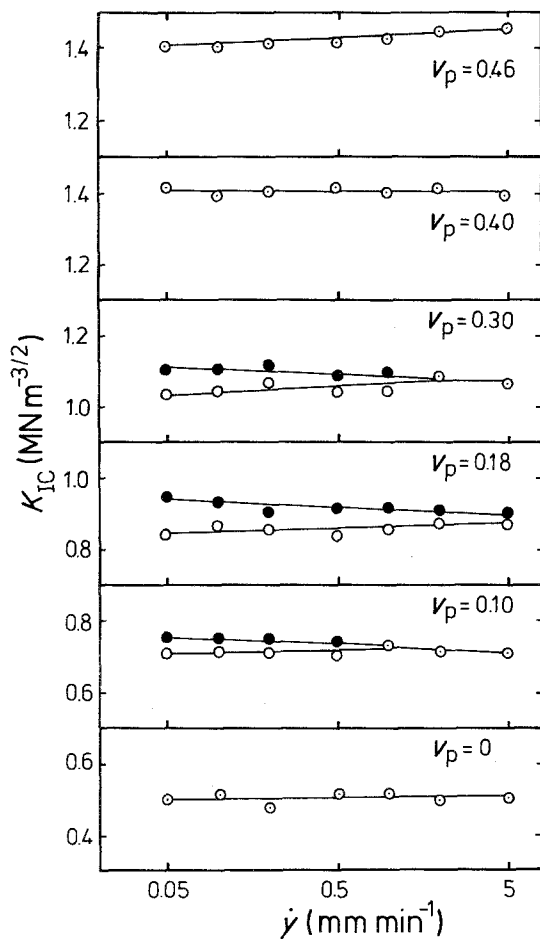


Figure 1 Variation of  $K_{IC}$  with crosshead speed,  $\dot{\gamma}$ , for different volume fractions of A187 treated,  $4.5 \mu\text{m}$  diameter particles. ● – crack initiation, ○ – crack arrest, and ○ – continuous propagation.

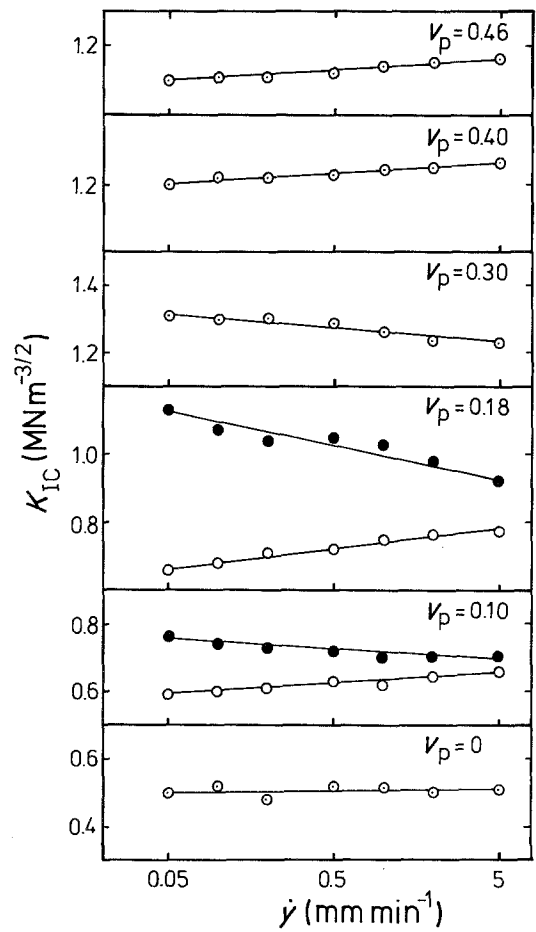


Figure 2 Variation of  $K_{IC}$  with crosshead speed,  $\dot{\gamma}$ , for different volume fractions of DC1107 treated,  $4.5 \mu\text{m}$  diameter particles. (The symbols have the same meaning as in Fig. 1).

### 3.2. Stress intensity factor

It can be seen from Figs. 1 and 2 that  $K_{IC}$  for both initiation and arrest tends to increase with an increasing volume fraction of particles for both types of pretreatment. The behaviour can be seen more clearly in Fig. 3 where  $K_{IC}$  is plotted against  $V_p$  for treated and untreated particles using a fixed crosshead speed of  $0.5 \text{ mm min}^{-1}$ . When the particles are treated with coupling agent (Fig. 3a)  $K_{IC}$  increases with increasing  $V_p$ . In the case of untreated particles  $K_{IC}$  increases with  $V_p$  for the large  $62 \mu\text{m}$  particles but it reaches a plateau level for the  $4.5 \mu\text{m}$  particles (Fig. 3b). For the particles treated with release agent (Fig. 3c)  $K_{IC}$  increases with  $V_p$  for the larger particles but reaches a peak value at  $V_p = 0.30$  and decreases with higher volume fractions of  $4.5 \mu\text{m}$  particles. Although this behaviour is rather complex it can be seen

that the highest values of  $K_{IC}$  are obtained for the highest volume fractions of the large particles – regardless of the surface pretreatment. The surface pretreatment seems to have only a secondary effect upon the value of  $K_{IC}$ .

### 3.3. Young's modulus

The dependence of the Young's modulus,  $E$ , of the composites containing treated and untreated particles upon  $V_p$  is shown in Fig. 4. The two curves are the upper and lower bounds of the calculations of Ishai and Cohen [14] – the lower bound corresponding to uniform displacement at the particle/matrix interface and the upper bound corresponding to uniform stress [1]. It can be seen that  $E$  generally increases with increasing  $V_p$  and that the points tend to fall closer to the uniform displacement, lower bound.

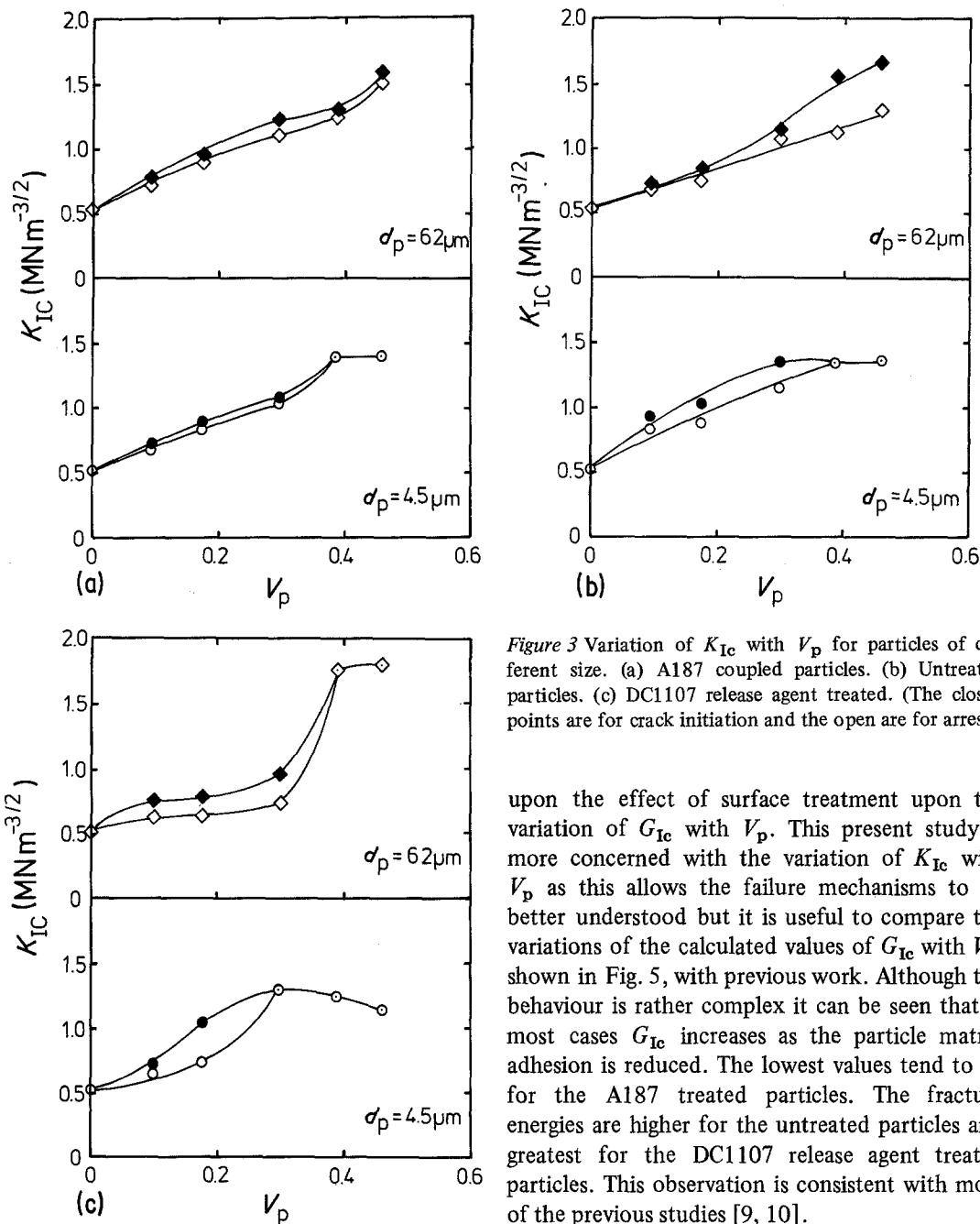


Figure 3 Variation of  $K_{IC}$  with  $V_p$  for particles of different size. (a) A187 coupled particles. (b) Untreated particles. (c) DC1107 release agent treated. (The closed points are for crack initiation and the open are for arrest).

upon the effect of surface treatment upon the variation of  $G_{IC}$  with  $V_p$ . This present study is more concerned with the variation of  $K_{IC}$  with  $V_p$  as this allows the failure mechanisms to be better understood but it is useful to compare the variations of the calculated values of  $G_{IC}$  with  $V_p$ , shown in Fig. 5, with previous work. Although the behaviour is rather complex it can be seen that in most cases  $G_{IC}$  increases as the particle matrix adhesion is reduced. The lowest values tend to be for the A187 treated particles. The fracture energies are higher for the untreated particles and greatest for the DC1107 release agent treated particles. This observation is consistent with most of the previous studies [9, 10].

A great deal of emphasis has been placed in the past upon both the increase in  $G_{IC}$  with reduction of adhesion and the positions of the maxima in plots of  $G_{IC}$  against  $V_p$ , which have both been used to interpret the mechanisms of propagation [9, 10]. However, the peaks in  $G_{IC}$  are more a result of the variation in the Young's modulus,  $E$ , with surface treatment and  $V_p$ , than any change in mechanism. It was shown in Section 3.2 that  $K_{IC}$  does not depend strongly upon surface pre-treatment and since  $G_{IC}$  is determined using

However, for all volume fractions and particle sizes the composites containing particles treated with release agents have significantly lower values of modulus than those treated with coupling agents. This has important implications for the calculations of  $G_{IC}$  and the analysis of crack propagation.

### 3.4. Fracture energy

Most previous studies [8–10] have concentrated

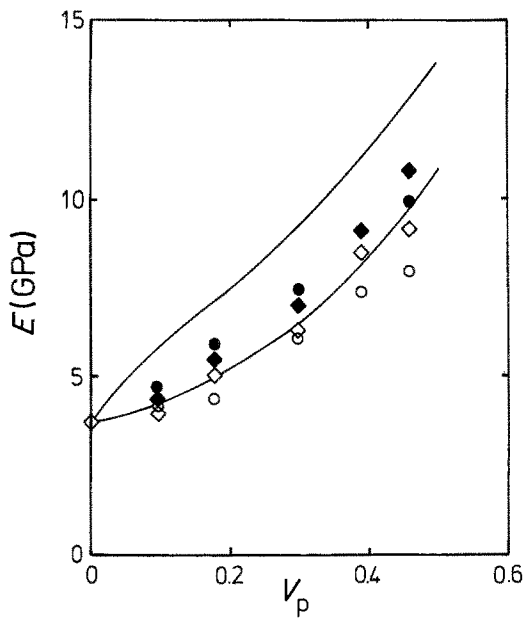


Figure 4 Variation of Young's modulus,  $E$ , with  $V_p$  for different particle diameters. The two lines are the upper and lower bounds of the theory of Ishai and Cohen [14] ● – A187 treated  $4.5\ \mu\text{m}$  particles, ○ – DC1107 treated  $4.5\ \mu\text{m}$  particles, ◆ – A187 treated  $62\ \mu\text{m}$  particles, and ◇ – DC1107 treated  $62\ \mu\text{m}$  particles.

Equation 1 most of the dependence of  $G_{Ic}$  upon surface pretreatment is due to the variation of  $E$ . Moreover, it was shown in Part 1 [1] that peaks in the variation of  $G_{Ic}$  with  $V_p$  can occur without any change in failure mechanism. In the analysis of crack propagation in Section 4 most of the emphasis is placed upon analysing the factors controlling  $K_{Ic}$  rather than  $G_{Ic}$ .

### 3.5. Fracture strength

For many practical purposes it is the fracture strength of the composites which is most important. Fig. 6 shows the variation in the ratio of the fracture strength of the composites to that of the unfilled matrix,  $\sigma_f/\sigma_0$  with  $V_p$ , for both particle sizes and pretreatments. The fracture strengths of the composites with A187 coupled particles falls slightly at low volume fractions but equals that of the pure resin above  $V_p \sim 0.4$ . The strengths of the composites containing DC1107 release agent treated particles fall rapidly as  $V_p$  increases. The behaviour is similar for both the  $4.5$  and  $62\ \mu\text{m}$  diameter particles. The strengths of the composites containing untreated particles lie between those of the A187 and DC1107 treated particles but tend to be closer to the strengths of composites containing release agent treated particles.

Previous work upon the strength of particulate composites has been explained by Nicolais and Nicodemo [4] who showed from simple geometrical considerations that

$$\sigma_f/\sigma_0 = 1 - 1.21V_p^{2/3} \quad (2)$$

when there is no adhesion between the particles and matrix. This equation is plotted as the lower lines in Fig. 6 and it can be seen that there is reasonable agreement between the DC1107 experimental data and the theoretical curve.

Nicolais and Nicodemo [4] suggested that the upper bound of the behaviour should be for the strength of the composite to equal that of the unfilled matrix ( $\sigma_f/\sigma_0 = 1$ ) as shown in Fig. 6. The data for the composites containing A187 particles are approximately the same as those for the unfilled matrix and tend to support this prediction but there is a systematic slight fall at low volume fractions and an increase at higher volumes of  $V_p$ .

There is an alternative way of viewing the behaviour since the fracture strength of an unnotched specimen is given by [2]

$$\sigma_f = K_{Ic}/(Ya_0)^{1/2} \quad (3)$$

where  $a_0$  can be thought of as the size of inherent flaws and  $Y$  is a geometrical factor. This means that  $\sigma_f$  depends upon both  $K_{Ic}$  and  $a_0$ . Since the addition of particles increases  $K_{Ic}$  (Fig. 3) then if  $a_0$  remained constant  $\sigma_f$  would be expected to increase with increasing  $V_p$ . Clearly the behaviour shown in Fig. 6 reflects a balance between the addition of particles increasing both  $K_{Ic}$  and  $a_0$ . With no or poor adhesion, the inherent flaw size increases rapidly as breakdown of the particle/matrix interface under stress will lead to large flaws. On the other hand, with good adhesion the interface remains intact and the presence of the particles produces a smaller increase in the flaw size.

### 3.6. Fractography

A large number of fracture surfaces were examined for the treated and untreated particles but only two representative micrographs are shown here. Tails were seen at low volume fractions but not at higher values of  $V_p$ . Fig. 7a shows a micrograph from a composite containing untreated  $4.5\ \mu\text{m}$  particles ( $V_p = 0.40$ ). The particles can be seen clearly and the crack seems to have propagated around their equators. This is quite different from the micrograph shown in Fig. 7b which is of an

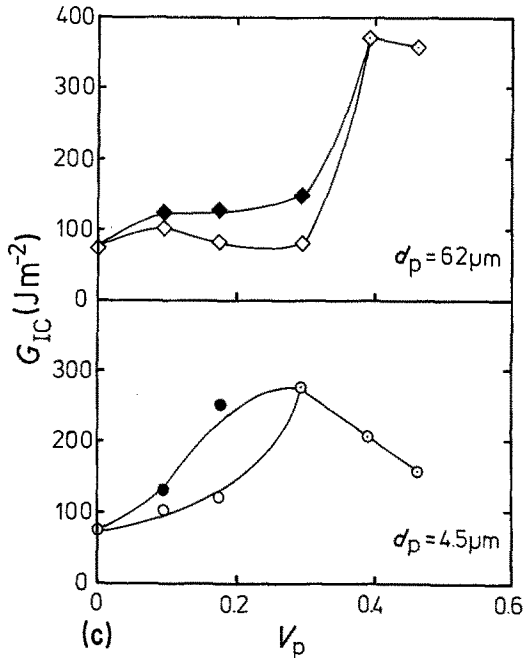
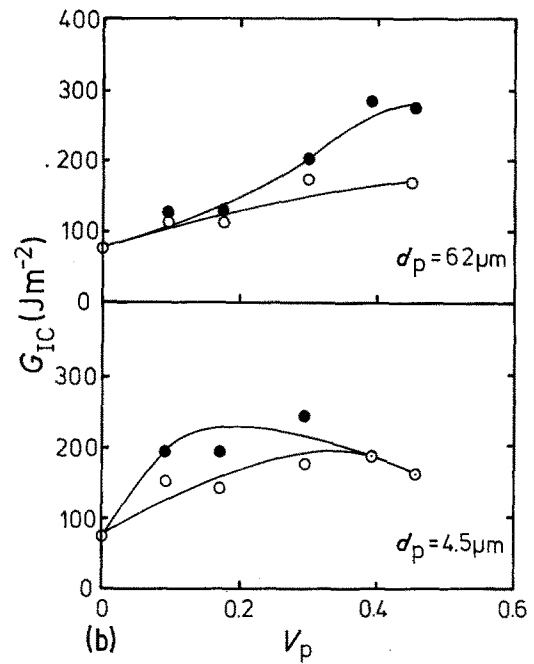
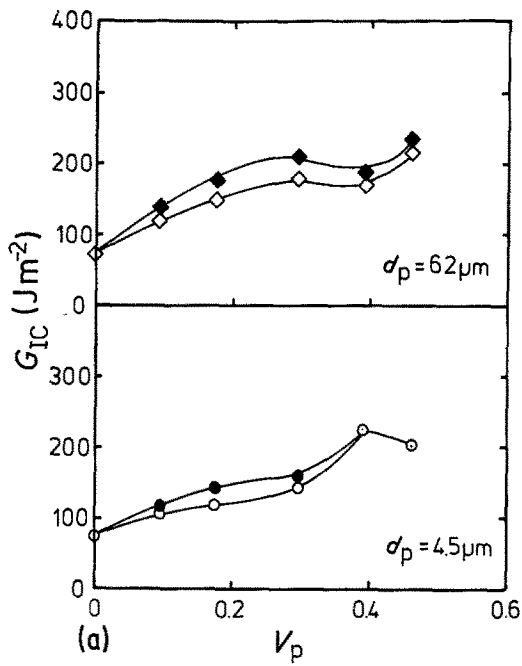


Figure 5 Variation of Fracture energy  $G_{IC}$  with  $V_p$  for different particle diameters. (a) A187 coupled particles. (b) Untreated particles. (c) DC1107 treated particles. (The closed points are for crack initiation and the open ones are for arrest).

agent treated particles were similar to those of composites with untreated particles.

#### 4. Crack propagation mechanisms

It was shown in the first part of this series [1] that crack propagation in composites containing untreated particles could be explained in terms of a combination crack-tip blunting and pinning. Observations in this present study have produced broadly similar results.

##### 4.1. Analysis of propagation

It was shown in Section 3.1 that unstable propagation in the composites could be caused by blunting, reflecting the rate dependence of the yield stress of the material [1, 12, 13]. The effect of blunting can be removed and the analysis simplified in the case of unstable propagation by extrapolating the  $K_{IC}$  data for initiation and arrest in Figs. 1 and 2 until the two lines meet. The values of  $K_{IC}$  so produced correspond to values for "sharp" unblunted cracks. These  $K_{IC}$  values can then be used to check the theoretical predictions of pinning of Evans and others [15–17] as described earlier [1]. This is done in Fig. 8, where

identical composition but contains particles treated with coupling agent. The particles are not so distinct and the epoxy resin matrix is seen to cover the particles, the crack having propagated through the matrix above or below the poles of the particles. Clearly, the crack propagation path is strongly affected by the improvement of adhesion at the particle/matrix interface. The appearance of the surfaces of composites containing release

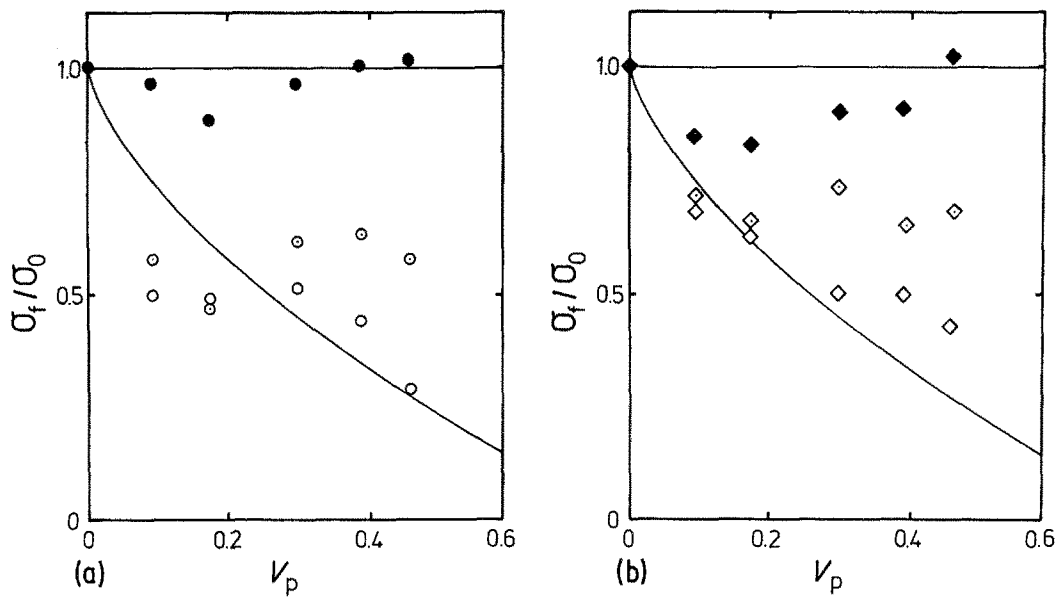


Figure 6 Variation of ratio of fracture stress of composite to that of the matrix,  $\sigma_f/\sigma_0$ , with  $V_p$ . The upper bound is for  $\sigma_f = \sigma_0$  and the lower bound is Equation 2. (a) 4.5  $\mu\text{m}$  diameter particles with different pretreatments  $\bullet$  – A187 treated,  $\circ$  – untreated and  $\odot$  – DC1107 treated. (b) 62  $\mu\text{m}$  diameter particles with different pretreatments  $\blacklozenge$  – A187 treated,  $\diamond$  – untreated and  $\odiamond$  – DC1107 treated.

the ratio of  $K_{Ic}$  (sharp) for the composite to  $K_{Ic}$  for the matrix,  $K_{Ic}/K_{Ic0}$  is plotted against  $d_p/D_s$ , the ratio of the average particle diameter to the interparticle separation. The solid lines are the theoretical predictions of Green *et al.* [17] for interacting and non-interacting elliptical secondary cracks. It can be seen that the data points for the coupled particles fall close to the theoretical line whereas there is more scatter for the particles treated with release agent and a tendency for them to fall below the lower curve. This implies that the efficiency of pinning is improved with the presence

of coupling agents but that pinning is not so efficient for the particles treated with release agent. This is consistent with the appearance of the fracture surface in Fig. 7b where the presence of A187 coupling agent ensures that there is no breakdown of the particle/matrix interface. It is likely that the breakdown of this interface will lead to a reduction in the efficiency of pinning as was also found for the composites containing untreated particles [1].

The situation can be summarized as follows. Improved adhesion tends to increase  $K_{Ic}$  because

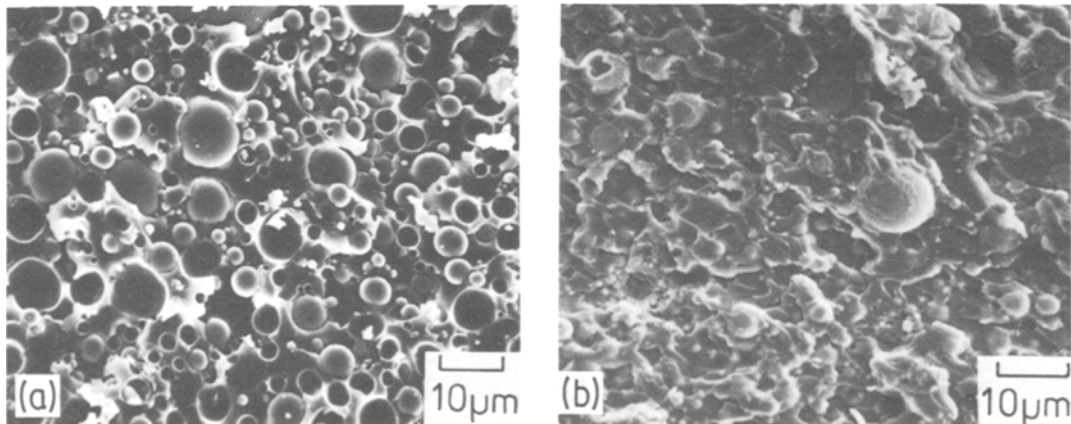


Figure 7 Fracture surfaces of composites containing 4.5  $\mu\text{m}$  diameter particles. (a) Untreated particles. (b) A187 treated particles.

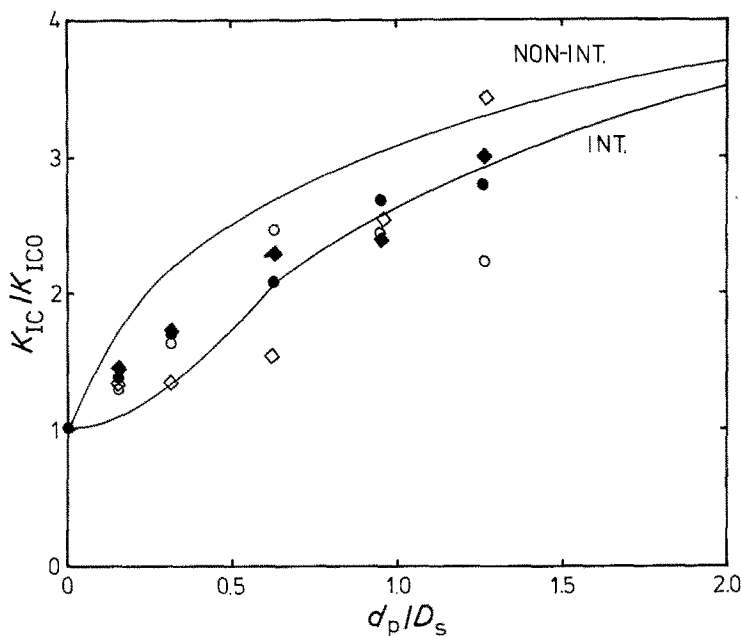


Figure 8 Variation of  $K_{IC}/K_{IC0}$  with  $d_p/D_s$  for different composites. The lines represent the theoretical predictions of Green *et al.* [17] for interacting and non-interacting elliptical cracks. (The symbols have the same meaning as in Fig. 4).

it improves the efficiency of pinning. However, decreased adhesion can also increase  $K_{IC}$  by causing more blunting to occur. Clearly, the overall behaviour can be quite complex with the dependence of the measured values of  $K_{IC}$  upon particle/matrix adhesion being controlled by a competition between blunting and pinning.

#### 4.2. Critical crack opening displacement criterion

It was shown earlier [1] that crack propagation in the composites containing untreated particles could be explained in terms of a critical crack opening displacement ( $\delta_c$ ) criterion, once the effect of blunting upon  $K_{IC}$  had been allowed for. If propagation occurs at a critical crack opening displacement,  $\delta_c$  then [1]

$$K_{IC} = E(\delta_c e_y)^{1/2} \quad (4)$$

where  $e_y$  is the yield strain of the material. If  $e_y$  is also constant then a plot of  $K_{IC}$  against  $E$  should be a straight line of slope  $(\delta_c e_y)^{1/2}$ . Fig. 9 is a plot of  $K_{IC}$  against  $E$  for the composites containing treated particles and the points lie close to the line through the origin with a slope of  $1.54 \times 10^{-4} \text{ m}^{1/2}$ . This is exactly the same slope as measured earlier for the composites with untreated particles [1]. This means that in the absence of blunting, crack propagation takes place at the same crack opening displacement ( $\delta_c \sim 0.4 \mu\text{m}$ ) regardless of surface pretreatment (as long as the yield strain remains unchanged). This should be

contrasted with the pinning analysis where the values of  $K_{IC}$  for the particles treated with release agent tend to fall below the theoretical line. However, the composites containing release agent treated particles also have values of modulus which are below the theoretical values (Fig. 4). Hence, these two effects tend to counteract each other and the data in Fig. 9 fall close to the theoretical line for both types of treatment.

#### 4.3. Fracture surfaces

It was shown in Fig. 7 that there is a difference in appearance between the fracture surfaces of

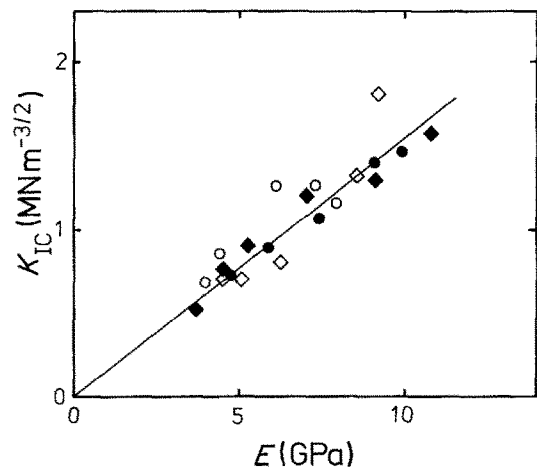


Figure 9 Dependence of  $K_{IC}$  upon  $E$  for the composites containing A187 and DC1107 treated particles. The symbols have the same meaning as in Fig. 4.



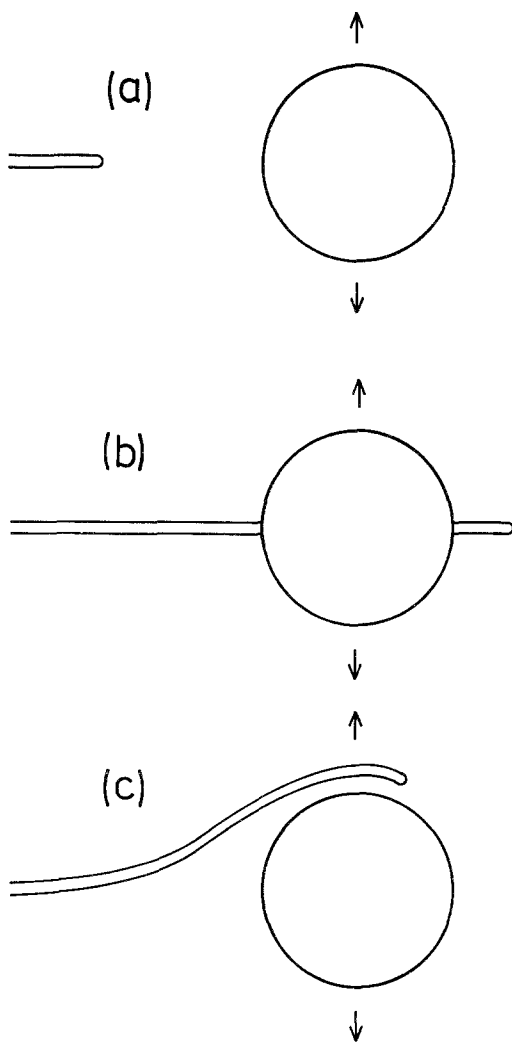


Figure 10 Schematic illustration of the path of a crack around a particle in a composite under stress. (a) Crack approaching particle. (b) Crack moving around equator or poorly-bonded particle. (c) Crack attracted to poles of well-bonded particle.

similar composites containing coupled and untreated particles. This can be explained by examining the local stresses around particles in a composite under an applied stress [18, 19] as shown in Fig. 10a. The strength of the interface has a profound effect upon the local stresses around the particles.

The case of debonded or poorly-bonded particles is similar to that of spherical holes where the maximum tensile stress is at the equators of the particles and holes [18, 19]. This means that the cracks propagating through the composite in Fig. 7a are attracted to the equator of the particle as shown in Fig. 10b. The fracture surface

therefore consists of hemispherical holes and the top surfaces of debonded particles (Fig. 7a). In the case of good bonding the situation is more complex and the maximum stress position is strongly dependent upon the elastic constants of the particles and the matrix [19]. Tirosch *et al.* [20] have investigated both theoretically and experimentally the transverse cracking of well-bonded fibres in composites which can be thought of as a two-dimensional analogy of the particle-filled composites under consideration. They were able to show that for a well-bonded fibre in a composite subjected to a transverse tensile stress the maximum stress is in the matrix above and below the poles of the fibre cross-section, the exact position depending upon the Poisson's ratio of the matrix [20]. Extending this analysis to particulate composites with well-bonded rigid particles implies that the maximum stresses should be in the matrix above and below the poles of the particles. This means that propagating cracks will be attracted to the poles of the particles rather than their equators as shown in Fig. 10c. Since the maximum stress is in the matrix the cracks will propagate through the matrix above or below the particles leaving a layer of epoxy resin covering the particles, exactly as can be seen in Fig. 7b.

#### 4.4. Overall fracture behaviour

It is worthwhile at this stage to consider what types of pretreatment produce composites with the best fracture properties. The values of  $K_{Ic}$  are not strongly dependent upon pretreatment. The fracture energies,  $G_{Ic}$  are the highest for the particles treated with release agent whereas the fracture strengths,  $\sigma_f$  are highest for composites containing particles treated with coupling agent. Clearly therefore, it is not possible to have high values of  $G_{Ic}$  and  $\sigma_f$  at the same time. For most purposes, it is the fracture strength which is important and since  $K_{Ic}$  is not strongly affected by surface treatment, composites containing particles treated with coupling agents will normally have the best mechanical properties.

#### 5. Conclusions

The effect of particle/matrix adhesion upon the fracture of a particle-filled epoxy resin composite has been studied in detail. The following observations have been made:

(i) The main mechanism of toughening is pinning and when this occurs a critical crack

opening displacement criterion can be applied.

(ii) The strength of the adhesion has only a small effect upon  $K_{Ic}$  but poor bonding causes an increase in  $G_{Ic}$  due to a reduction in the Young's modulus,  $E$ .

(iii) The strength of the adhesion has a strong effect upon the fracture strength,  $\sigma_f$  and the fracture surface appearance. With poor bonding  $\sigma_f$  falls sharply as the volume fraction of particles is increased whereas with good bonding  $\sigma_f$  remains approximately constant.

(iv) For most purposes, the best mechanical properties are obtained for composites treated with coupling agents where the particle/matrix adhesion is good.

### Acknowledgements

This project was supported partly by a Research Grant from the Science and Engineering Research Council. The authors are grateful to Dr A. J. Kinloch for useful discussion.

### References

1. J. SPANOUDAKIS and R. J. YOUNG, *J. Mater. Sci.* **19** (1984) 473.
2. A. J. KINLOCH and R. J. YOUNG, "Fracture Behaviour of Polymers" (Applied Science, London, 1983), Chap. 11.
3. S. SAHU and L. J. BROUTMAN, *Polym. Eng. Sci.* **12** (1972) 91.

4. L. NICHOLAIS and L. NICODEMO, *ibid.* **13** (1973) 469.
5. J. LEIDNER and R. T. WOODHAMS, *J. Appl. Polym. Sci.* **18** (1974) 1639.
6. J. SPANOUDAKIS, "Fracture in Particle-Filled Epoxy Resins", PhD thesis, University of London (1981).
7. S. K. BROWN, *Brit. Polym. J.* **14** (1982) 1.
8. J. C. HAMMOND and P. V. QUALE, 2nd International Conference on 'Yield, Deformation and Fracture', Cambridge, (Plastics and Rubber Institute, London, 1973).
9. L. BROUTMAN and S. SAHU, *Mater. Sci. Eng.* **8** (1971) 98.
10. S. K. BROWN, *Brit. Polym. J.* **12** (1980) 24.
11. R. A. GLEDHILL, A. J. KINLOCH, S. YAMINI and R. J. YOUNG, *Polymer* **19** (1978) 574.
12. S. YAMINI and R. J. YOUNG, *J. Mater. Sci.* **15** (1980) 1823.
13. A. J. KINLOCH and J. G. WILLIAMS, *ibid.* **15** (1980) 987.
14. O. ISHAI and L. J. COHEN, *Int. J. Mech. Sci.* **9** (1967) 539.
15. A. G. EVANS, *Phil. Mag.* **26** (1972) 1327.
16. D. J. GREEN, P. S. NICHOLSON and J. D. EMBURY, *J. Mater. Sci.* **14** (1979) 1413.
17. *Idem*, *ibid.* **14** (1979) 1657.
18. A. K. KHAUND, V. D. KRSTIC and P. S. NICHOLSON, *ibid.* **12** (1979) 2269.
19. J. N. GOODIER, *J. Appl. Mech.* **1** (1933) 39.
20. J. TIROSH, E. KATZ, G. LIFSCHUETZ and A. S. TETELMAN, *Eng. Fract. Mech.* **12** (1979) 267.

Received 10 May  
and accepted 26 May 1983